Research Paper

Drug Release Kinetics and Transport Mechanisms from Semi-interpenetrating Networks of Gelatin and Poly(ethylene glycol) diacrylate

Yao Fu,[1] and Weiyuan John Kao[1,2,3]

Purpose. To elucidate the key parameters affecting solute transport from semi-interpenetrating networks (sIPNs) comprised of poly(ethylene glycol) diacrylate (PEGdA) and gelatin that are partially crosslinked, water-swellable and biodegradable. Effects of material compositions, solute size, solubility, and loading density have been investigated.

Materials and Methods. sIPNs of following gelatin/PEGdA weight-to-weight ratios were prepared: 10:15, 10:20, 10:30, 15:15, 20:15. Five model solutes of different physicochemical properties were selected, *i.e.* silver sulfadiazine (AgSD), bupivacaine hydrochloride (Bup), sulfadiazine sodium (NaSD), keratinocyte growth factor (KGF), and bovine serum albumin conjugated with fluorescein isothiocyanate (BSA-FITC). Release studies were performed and the results were analyzed using three hydrogel based common theories (free volume, hydrodynamic and obstruction).

Results. The release kinetics of model solutes was influenced by each factor under investigation. Specifically, the initial release rates and intra-gel diffusivity decreased with increasing PEGdA content or increasing solute molecular weight. However, the initial release rate and intra-gel diffusivity increased with increasing gelatin content or increasing solute water solubility, which contradicted with the classical hydrogel based solute transport theories, *i.e.* increasing polymer volume leads to decreased solute diffusivity within the gel.

Conclusion. This analysis provides structure-functional information of the sIPN as a potential therapeutic delivery matrix.

KEY WORDS: diffusion; gelatin; poly(ethylene glycol) diacrylate; semi-interpenetrating network.

INTRODUCTION

A semi-interpenetrating network (sIPN) comprised of photocrosslinked poly(ethylene glycol) diacrylate (PEGdA) and a naturally derived macromolecule gelatin has been developed (1). Designed for wound healing, the sIPNs are photocrosslinked *in situ* under physiological conditions, enabling complete wetting of the wound bed, even in the presence of complex 3-D topography (2). sIPNs are distinguishable from blends, block copolymers, and graft copolymers in two ways: firstly, the sIPN swells but does not dissolve in solvents, and secondly, creep and flow are suppressed (3). Bearing similarities to hydrogels, such as crosslinked matrices, high water capacity, and swelling ability, the sIPN system is only partially crosslinked, which makes it more complex, more heterogeneous and less rigid than classical hydrogel systems. Previous studies revealed that the sIPN (gelatin:PEGdA 10:15 w/w) had a 30-fold higher Young's modulus compared to the 0.1% glutaraldehyde crosslinked gelatin hydrogel and that sIPNs with higher gelatin content showed significantly higher Young's modulus (4). Incorporating crosslinked PEG matrices enhances protein resistance and maintains the mechanical stability (5). It also allows the mesh sizes of the sIPN system to be varied by varying the amount of PEG component in the formulation, which may further influence solute transport out of the sIPNs. The incorporation of gelatin component presents elasticity and biodegradability to the network. Increasing the gelatin content, a significantly higher Young's modulus has been observed (4). Moreover, the gelatin backbone has modification sites (lysyl residue) that can be grafted with PEG linker and further conjugated with bioadhesive peptide sequences, such as Arg-Gly-Asp (RGD) and Pro-His-Arg-Ser-Asn (PHRSN) (6), to mimic the extracellular matrix and act as a platform for wound healing. The sIPN has material properties, including moisture absorbance, high tensile strength and elasticity, tissue integration and adhesion, and favorable tissue response, that make it a potential wound-dressing material (7,8). *In vivo* studies have demonstrated that the *in situ* photopolymerized sIPN is a comparable and viable treatment for both partial-thickness porcine wounds and full-thickness rodent wounds (9,10). In addition, drug molecules can be directly incorporated into the polymer solution prior to polymerization rather than through equilibrium partitioning, which allows control over loading density. Drugs that possess poor water solubility can also be loaded in sIPNs *i.e.* fine drug particles with poor aqueous

[1] School of Pharmacy, University of Wisconsin-Madison, 777 Highland Ave., Madison, Wisconsin 53705, USA.

[2] Department of Biomedical Engineering, College of Engineering, University of Wisconsin-Madison, Madison, Wisconsin 53705, USA.

[3] To whom correspondence should be addressed. (e-mail: wjkao@pharmacy.wisc.edu)

solubility are suspended in the polymer solution and homogeneously distributed in the sIPN matrix after photopolymerization.

Per different clinical requirements, different release profiles are preferred. Thus, understanding the mechanism of solute transport out of sIPNs is critical. The three main forces that drive solute transport in hydrogels include a penetrant concentration gradient, a polymer stress gradient and osmotic forces (11). Fickian diffusion plays a dominant role for non-swelling controlled delivery systems, where polymer chain relaxation rate is slow. However, Fickian diffusion alone cannot explain the solute transport from swelling controlled delivery systems, where Case II transport is observed (11). Being partially crosslinked, water-swellable and biodegradable, there are multiple driving forces controlling solute transport out of the sIPNs. Therefore, it is necessary to characterize the contributing factors of sIPN components on the release kinetics of solutes by investigating the effect of each material component separately. Five model compounds were selected based on the molecular weight, structure, size, water solubility, and clinical utility, which not only explored the effect of solute physicochemical properties on their transport kinetics but also demonstrated the sIPN system as a potential carrier to deliver newly identified therapeutic factors, especially proteins and peptides. The Ritger-Peppas release model was applied to the experimental release data to gain insight into the major driving forces behind solute transport from sIPNs. Furthermore, the relationship between polymer volume fraction and the diffusivity reduction of solutes within the matrix was tested based upon three hydrogel diffusion models.

MATERIALS AND METHODS

Gelatin (type A: from porcine skin, 300 bloom), poly (ethylene glycol) diacrylate (PEGdA, MW 575 Da), 2,2-dimethoxy-2-phenyl-acetophenone initiator (DMPA), phosphoric acid (HPLC grade), methoxy poly(ethylene glycol) (mPEG, MW 2 kDa), silver sulfadiazine (AgSD), bupivacaine hydrochloride (Bup), sulfadiazine sodium (NaSD), and bovine serum albumin conjugated with fluorescein isothiocyanate (BSA-FITC) were purchased from Sigma-Aldrich. Keratinocyte growth factor (KGF) was obtained from R&D systems. RPMI 1640 culture media was purchased from Gibco, Invitrogen. All other commercial reagents were received from Fisher Scientific and used without further purification.

Synthesis of sIPNs, PEG-hydrogel and Gelatin-Hydrogel

sIPNs of different gelatin-PEGdA weight ratios were prepared following previously described procedures (4,6). Gelatin dissolved in ddH$_2$O was heated to approximately 45°C and mixed with PEGdA and 0.1% DMPA (w/v). The mixture was poured over Teflon® molds (disk; surface area, 0.75 cm^2; thickness, 1.4 mm) and crosslinked under UV light with CF1000 LED (λ_{max}=365 nm, Clearstone Technologies) for 3 min. sIPN formulations included the following gelatin/PEGdA weight-to-weight ratios 10:15, 10:20, 10:30, 15:15, and 20:15. mPEG modified gelatin was synthesized and the modified sIPNs were prepared as described above (6). To elucidate the impact of each

component, PEG-only hydrogels (15% PEGdA, w/v) were prepared following the same protocol as above but in the absence of gelatin.

In Vitro Release Kinetics of Selected Compounds

Model solutes were first mixed with gelatin and PEGdA solution prior to polymerization and synthesized as described previously. The physicochemical properties of five solutes were summarized in Table I. AgSD and Bup were loaded both separately and concurrently into sIPN disks. Drug-loaded sIPNs were placed in individual glass vials containing 5 ml 1× PBS at pH 7.4 or RPMI 1640 culture media at 37°C. At a given time, 5 ml release media was removed and replaced with fresh release media to maintain the sink condition. Aliquots of samples were further analyzed to determine the concentration of drug released at each time point. The amount of drug released was calculated by concentration × volume (×5 ml). The amount at each time point was added to the amount at all previous points to obtain the cumulative release amount (m_t), which was then divided by the original mass of drug loaded (m_0) to obtain the cumulative release fraction (m_t/m_0). Assuming homogeneous distribution of drug molecules in the unpolymerized material solution, the original mass of drug loaded (m_0) was estimated using Eq. 1.
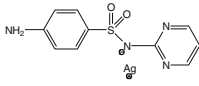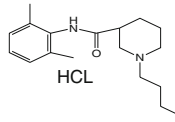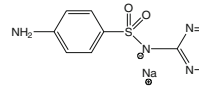
$$m_0 = A_{total} \cdot \frac{V_{disk}}{V_{total}} \qquad (1)$$

In Eq. 1, A_{total} represents the total amount of drug added to the polymer solution. V_{disk} is the volume of polymer solution applied to each Teflon® mode and V_{total} is the total volume of polymer solution.

Analytical Methods

To simultaneously quantify the release of AgSD and Bup, an HPLC-based analytical method was developed. The HPLC system consisted of Model 306 pumps (Gilson) and a variable-wavelength UV detector (Model UV/Vis-155, Gilson). Separations were performed on a reverse phase column (C$_{18}$, 5μm pore size, 4.6×250 mm, Waters). The mobile phase consisted of solvent A, 0.1% (v/v) H$_3$PO$_4$ and solvent B, acetonitrile containing 0.1% H$_3$PO$_4$ (v/v). A gradient elution was carried out as follows: 15% (v/v) solvent B was used for 0–5 min, then linearly increased to 85% (v/v) for 5–25 min and maintained for another 5 min. The injection volume was 200 μl and eluted at a flow rate of 1.0 ml/min at 23°C. The eluents were monitored at 210 nm and 254 nm. Samples were pre-filtered through a 0.45μm membrane filter (Whatman) before injection into the HPLC column. Due to the poor water solubility of AgSD, a standard stock solution of AgSD was prepared at a concentration of 1 mg/ml in 10% NH$_3$·H$_2$O (17). Thus, the HPLC analytical method quantified the concentration of sulfadiazine (SD) group instead of the AgSD complex. AgSD standards were prepared at concentrations of 1.625, 3.125, 6.25, 12.5, 25, 50, 100, 200μg/ml. Bup standards were prepared similarly using distilled water as solvent. The calibration curve was obtained by linear regression of the peak-area *vs.* concen-

Table I. Physicochemical Properties of Model Compounds

Properties	AgSD [a]	Bup [b]	NaSD [c]	KGF [d]	BSA-FITC [e]
Chemical formula	$C_{10}H_9AgN_4O_2S$	$C_{18}H_{28}N_2O \cdot HCl$	$C_{10}H_9N_4NaO_2S$	-	-
Chemical structure				-	-
Molecular weight (Da)	357.1	324.9	272.3	19 k	66 k
pKa/IEP	6.1 [f]	8.1 [f]	6.5 [f]	3.5 [g]	5.0 [g]
Hydrodynamic radius r_s (Å)	6.15	5.15	4.0	19.7	36.5
Water solubility	Insoluble	Soluble	Soluble	Soluble	Soluble
Loading density (per disk)	1000 μg	1000 μg	2000 μg	10 ng	1000 μg

[a] taken from (12)

[b] taken from (13)

[c] taken from (14)

[d] taken from (15)

[e] taken from (16)

[f] pKa

[g] isoelectric point

tration (AgSD, $Y = 356383X - 233195$, $R^2 = 0.9998$; Bup, $Y = 492685X - 644029$, $R^2 = 0.9995$). The linearity range was between 3.125–200 μg/ml for both AgSD and Bup. To quantify NaSD concentration, the UV absorbance of samples was measured at 254 nm using a spectrophotometer (Genesys 8, Thermospectronic). Linearity range was between 3.9–62.5 μg/ml ($Y = 0.0333X$, $R^2 = 0.9906$). To quantify KGF, commercially available anti-human KGF enzyme-linked immunosorbent assay (R&D System) kits were used. KGF release samples were lyophilized and reconstituted in 0.5 ml ddH$_2$O. The detection range of the KGF ELISA assay was 15–2000 pg/ml. To quantify BSA-FITC, the concentration of BSA-FITC was determined by spectrofluorometric analysis (Thermo-Spectronic AB/2 luminescence spectrometer) with excitation and emission wavelength of 495 and 520 nm, respectively ($Y = 0.2011X - 0.0785$, $R^2 = 0.9995$). The linearity range was between 0.625–20 μg/ml. Samples were pre-filtered and diluted prior to analysis.

Mathematical Analysis

Analysis of drug release kinetics from sIPNs and PEG-only hydrogels was performed by calculating the diffusion coefficients within the gel, D_E and D_L, using the early-time (Eq. 2) and late-time (Eq. 3) approximation equations, respectively. Both Eqs. 2 and 3 are approximations of the equation obtained when solving Fick's second law of diffusion under initial and boundary conditions equivalent to those tested in this work (18):

$$\frac{M_t}{M_\infty} \cong 4\left(\frac{D_E t}{\pi \delta^2}\right)^{0.5} \tag{2}$$

$$\frac{M_t}{M_\infty} = 1 - \frac{8}{\pi^2} \exp\left(\frac{-\pi^2 D_L t}{\delta^2}\right) \tag{3}$$

Where M_t/M_∞ is the cumulative fractional drug release, t is the release time, D_E and D_L are the corresponding diffusion coefficients and δ is the diffusion distance, *i.e.* half the thickness of the disk, which is 0.7 mm. The data points used for fitting eqs. 1 and 2 were defined as 0–6 h for early-time equation and 6–24 h for late-time equation.

$$\frac{M_t}{M_\infty} = kt^n \tag{4}$$

The Ritger-Peppas equation (Eq. 4) was employed for evaluating the drug release mechanism. M_t/M_∞ is the cumulative fractional drug release, k is a kinetic constant, t is the release time and n is the diffusional exponent related to transport mechanism (19). For a slab-like delivery device, when $n = 0.5$, drug transport is driven by Fickian diffusion (19). When $n = 1$, Case II transport is observed, leading to zero-order release (19). When $0.5 < n < 1$ anomalous transport

occurs involving both Fickian diffusion and polymer chain relaxation (19).

The reduction in diffusivity of drug molecules in the sIPN was expressed as the ratio of the diffusivity in the sIPN to the diffusivity in the water, D_E/D_0 or D_L/D_0 (20). D_0 was roughly correlated to size and calculated according to Stokes-Einstein equation (Eq. 4). Small molecules can be considered as spheres and the molecular radius can be estimated by Eq. 6 (21).

$$D_0 = \frac{kT}{6\pi\eta r_s} \qquad (5)$$

$$r_s = \left(\frac{3M\nu_\rho}{4\pi N_0}\right)^{\frac{1}{3}} \qquad (6)$$

In Eq. 5, k is Boltzmann constant, T is the temperature assuming at room temperature (25°C), and η is the water viscosity at the temperature T and r_s is the Stokes radius of solute. In Eq. 6, M is the molecular weight, N_0 is Avogadro's number, and ν_ρ is the specific gravity. Eq. 6 was used to estimate the molecular radii of AgSD, Bup, NaSD and KGF (Table I).

D_E/D_0 or D_L/D_0 data were fit to three hydrogel-based solute diffusion models using a nonlinear regression algorithm (Origin 8.0). The applicability of the model was determined by analysis of the sum of squares of the residuals (SSR), the correlation coefficient (R^2), and the fitted parameters (22).

Statistical Analysis

Statistical analysis of all release data was performed using paired Student's t-test at the $p < 0.05$ level. All experiments were repeated in triplicates and the data was represented as the mean ± standard deviation (S.D.).

RESULTS

Release Kinetics of AgSD, Bup and NaSD

The release of single loaded AgSD and Bup was quantified over 7 days. For most sIPN formulations, SD or AgSD showed a near zero-order initial release between 0 and 12 h followed by a second release phase with decreased release rate and the cumulative maximum release reached near constant after 24 h (Fig. 1A). Comparison between sIPNs of varying PEGdA content showed that less SD or AgSD was released with increasing PEGdA weight percentage. The increased crosslinking density and smaller mesh size as a result of increasing PEGdA weight percentage may prevent the diffusion of SD out of the sIPN matrix (16). With increasing gelatin weight percentage, the average cumulative release fraction of SD was increased within the first 8 h (Fig. 2A). Significant differences between sIPN and PEG-only hydrogel groups showed significantly higher fractional release from sIPNs than from PEG-only hydrogels ($p < 0.05$) (Fig. 2A), suggesting that gelatin dissolution might promote the solute release. Compared to the release behavior of SD, single-loaded water-soluble Bup displayed an extremely rapid 'burst effect' release from 0 to 6 h with maximum cumulative
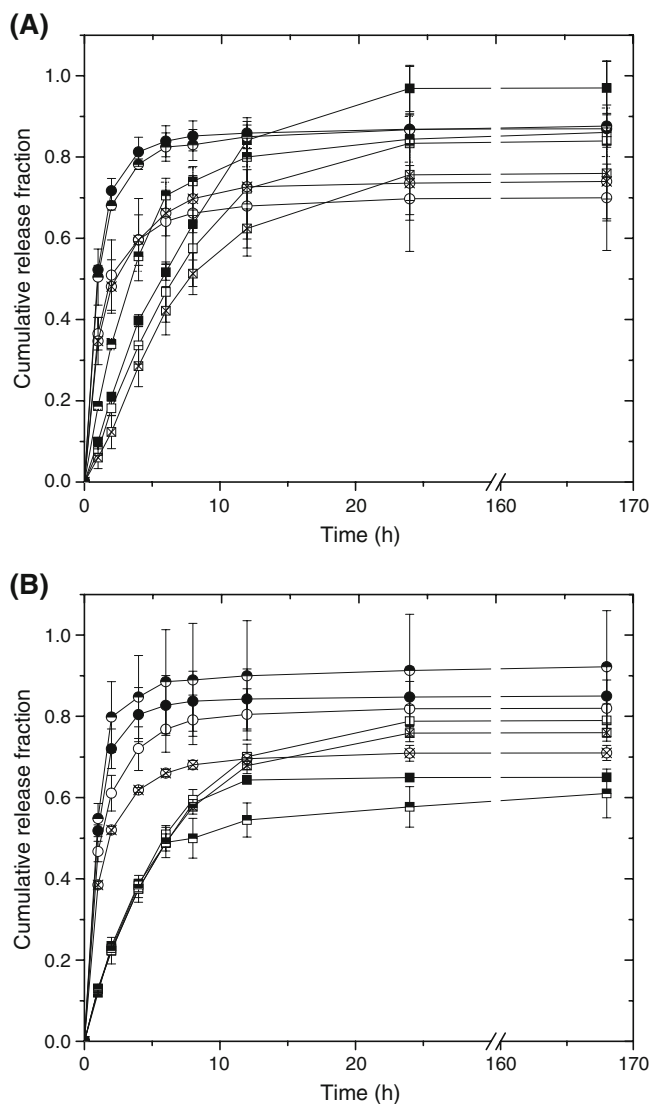

Fig. 1. Effects of PEGdA content and mPEG-modified gelatin on SD and Bup release from (A) Single loading sIPNs and (B) Concurrent loading sIPNs. SD from sIPNs of PEGdA content (w/v) 15% (—■—), 20% (—□—), 30% (—⊠—); SD from mPEG modified sIPN (—■—); Bup from PEGdA content (w/v) 15% (—●—), 20% (—○—), 30% (—⊗—); Bup from mPEG modified sIPN (—◖—). Data represented as average ± S.D. ($n=3$).

fractional release of 70–100% (Figs. 1A, and 2A). PEGdA and gelatin weight percentages both had impacts on the cumulative release fraction of Bup. The average cumulative release fraction was decreased for Bup with increasing PEGdA weight percentage. However, more Bup was released with increased gelatin weight percentage. With respect to mPEG modified sIPNs (Fig. 1A), SD and Bup showed relatively higher initial release rates than unmodified sIPNs (Table II).

The aim of concurrent loading was to delineate the possible drug-drug interaction that could impact the release kinetics of each compound. Compared to single loading release results, concurrent loading did not show significant differences in the overall release behavior of Bup in terms of initial release rates ($p > 0.05$) (Table II). But for AgSD, single-loaded 15% PEGdA group reached around 100% cumulative
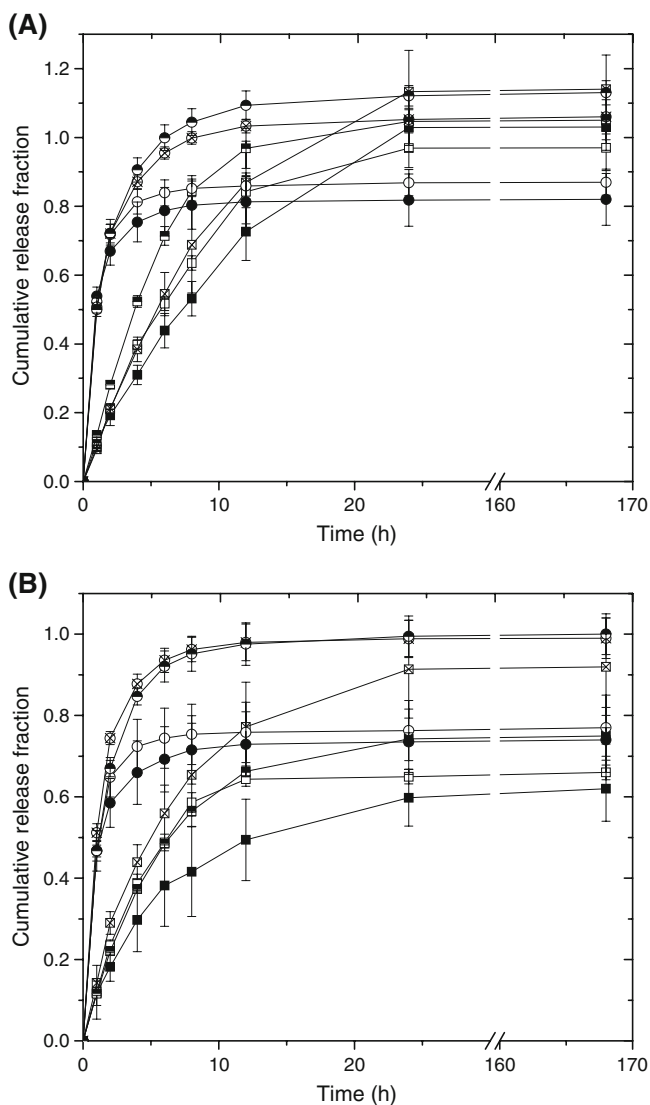
Fig. 2. Effects of gelatin content on SD and Bup cumulative release fraction from (A) Single loading and (B) Concurrent loading sIPNs and PEG-only hydrogels. SD from sIPNs of gelatin content (w/v) 0% (——■——), 10% (——□——), 15% (——⊠——), 20% (——■——); Bup from gelatin content (w/v) 0% (——●——), 10% (——○——), 15% (——⊗——), 20% (——❂——). Data represented as average ± S.D. (*n*=3).

release percentage over 168 h while only around 60% when loaded with Bup (Fig. 1B). This decreased cumulative SD release could be related to drug loading errors as a result of inhomogeneous distribution of drugs due to the low water solubility of AgSD. sIPNs of varying PEGdA content showed no statistically significant differences within first 8 h (*p*>0.05), suggesting that the PEGdA content had a less significant impact on the release behavior of AgSD from concurrent loaded sIPNs than from single loaded sIPNs in the early time points (Fig. 1B). Varying the gelatin weight percentage led to AgSD and Bup release behaviors similar to that observed with single loaded sIPNs as increased gelatin weight percentage led to increased cumulative fractional release (Fig. 2B). mPEG modified sIPN release results were not statistically different from the unmodified sIPNs but showed slightly higher initial release rate (Table II).

To address whether the differences in release patterns between AgSD and Bup was due to the solubility differences of the two molecules, a water-soluble molecule NaSD was employed. Two release media, PBS and RPMI 1640 culture media, were used. Though some differences in terms of maximum release percentage were observed, no significant differences were observed in the initial release rate of NaSD between PBS and RPMI 1640 within 6 h (*p*>0.05) (Fig. 3), illustrating that release media was not a major impacting factor in this case. NaSD displayed a different release behavior from AgSD, but similar to the release profile of Bup, where approximately 50% was released in the first hour. As shown in Table III, all three model solutes mentioned above displayed the similar relationship between PEGdA/gelatin content and their release kinetics from single-loaded sIPNs.

Release Kinetics of KGF and BSA-FITC

KGF, a water-soluble protein, yielded a significantly different release behavior compared to small molecules (Fig. 4). KGF showed a slight burst release from 0 to 6 h, due to the release of surface associated KGF. Relatively low maximum cumulative release was observed, around 2–15%. Protein denaturation, aggregation, or interaction with the PEG diacrylate may account for the incomplete protein release. Similar to previous release results, increasing PEGdA weight percentage caused a decrease in drug release fraction while an increased drug release fraction was observed when increasing gelatin weight percentage.

Table II. Initial Normalized Release Rates (µg/h) from sIPNs and PEG Hydrogels at 37°C

Solute	Type of loading	MW (Da)	Formulations						
			1[a]	2[a]	3[a]	4[a]	5[a]	6[a]	7[a]
AgSD	Single	357.1	99.8±6.3	85.1±8.2	71.8±3.5	96.8±6.6	131.0±10.3	136.5±9.4	75.4±5.1
	Concurrent	357.1	96.2±4.5	94.0±6.9	92.0±5.8	109.0±7.8	92.3±4.2	92.0±5.8	71.6±5.4
Bup	Single	324.9	358.8±20.6	254.7±11.5	240.7±10.7	360.4±8.5	360.8±8.8	340.4±12.4	334.6±14.6
	Concurrent	324.9	360.0±15.2	305.4±19.3	260.2±7.7	372.2±12.9	334.8±14.5	399.2±17.2	292.6±13.6
NaSD	Single	273.3	625.8±16.9	619.1±22.4	448.4±11.6	776.8±28.7	881.5±33.4	-	808.4±39.4
KGF	Single	19 k	0.1±0.012	0.07±0.005	0.03±0.002	0.11±0.014	0.12±0.011	-	0.04±0.009
BSA-FITC	Single	66 k	51.0±4.1	40.5±5.4	29.4±3.8	46.1±2.5	100.6±8.2	-	66.4±7.2

[a], sIPN of gelatin/PEGdA w/w: 1, 10:15; 2, 10:20; 3, 10:30; 4, 15:15; 5, 20:15; 6, sIPN of mPEG modified gelatin/PEGdA w/w 10:15; 7, PEG-only hydrogel of 15% w/v PEGdA. Data represented as mean ± S.D. (*n*=3).
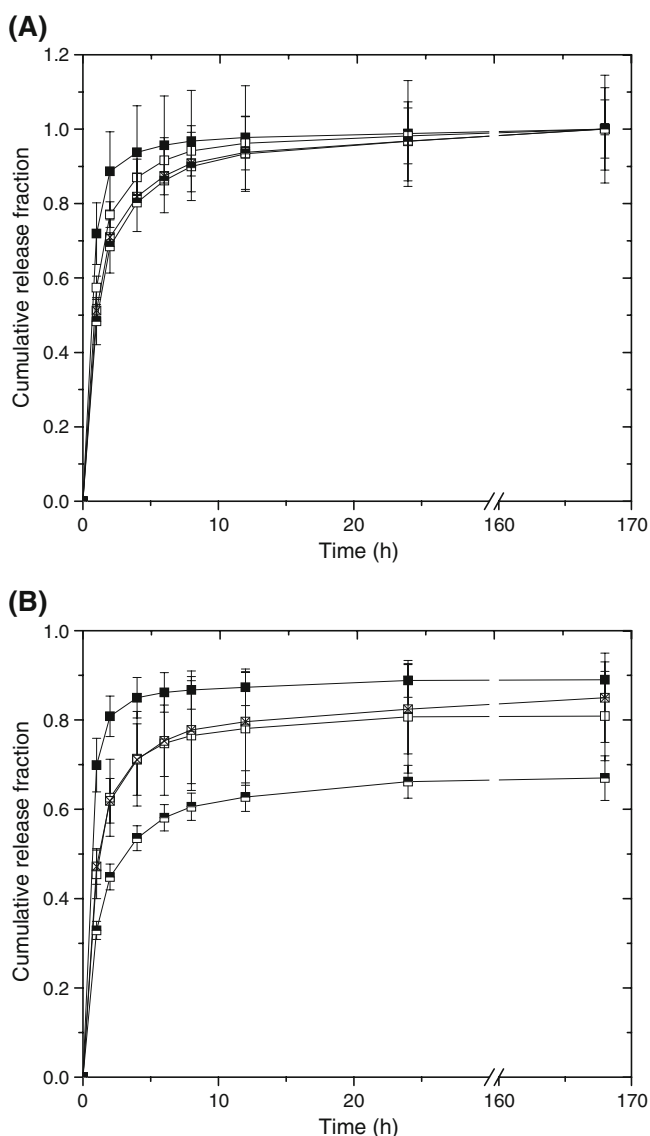
(A)

(B)

Fig. 3. Effects of PEGdA content on NaSD release fraction from sIPNs in (A) PBS and (B) RPMI 1640. 15% w/v PEG-only hydrogel (——■——), sIPNs of gelatin/PEGdA w/w ratios 10:15 (——□——), 10:20 (——⊠——), 10:30 (——■——). Data represented as average ± S.D. (*n*=3).
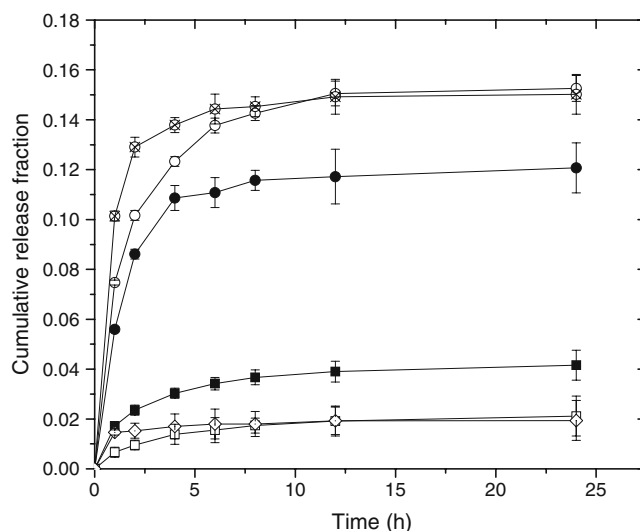

Fig. 4. Effects of PEGdA and gelatin content on KGF cumulative release fraction from sIPNs. sIPNs of gelatin/PEGdA w/w ratios 10:15 (——●——), 15:15 (——○——), 20:15 (——⊠——), 10:20 (——■——), 10:30 (——□——), 15% w/v PEG-only hydrogel (——◇——). Data represented as average ± S.D. (*n*=3).

To further examine the phenomenon behind the low cumulative release of KGF, BSA-FITC was selected. BSA-FITC also exhibited a biphasic release pattern with an initial release phase from 0 to 12 h and a second phase from 12 to 168 h (Fig. 5). In contrast to previous hydrophilic model

Table III. Summary of Factors That Influence Release Kinetics

Material and solute factors	Initial release rate	Fractional release
PEGdA weight percentages in sIPN ↑	↓	↓
Gelatin weight percentages in sIPN ↑	↑	↑
Solute molecular size ↑	↓	↓
Solute water solubility ↑	↑	↑

solutes, BSA-FITC showed a slight burst effect followed by a sustained release through 168 h. This could be explained by the relatively large molecular size of BSA-FITC. With higher PEGdA content, BSA-FITC release was decreased corresponding to the results observed with other model compounds. In contrast, more BSA was released from the sIPN disks when increasing gelatin content. The release profile of BSA-FITC from sIPN with the highest content of gelatin (20%, w/v) showed a sigmoid release curve. During the initial release phase, this sIPN group had the highest total polymer fraction (35%, w/v) and as a result, presented the most barriers for solute transport. Although gelatin dissolution seemed to enhance the release rate of solutes, the delayed burst effect could also be due to the time-lag related to gelatin dissolution. In comparison to small molecular weight solutes, KGF and BSA-FITC showed much smaller initial release rates (Table II), and as a result, increasing the solute molecular weight will lead to decreased release rate and cumulative release fraction (Table III).

Mathematical Analysis

Mathematical Analysis of the Drug Release Kinetics

In this study, we sought to apply the release data to the theoretical models and to elucidate the mechanism behind release kinetics. D_E values of small molecules were on the order of 10^{-8} cm^2/s while the D_E values were on the order of 10^{-9}–10^{-11} cm^2/s for proteins (Table IV). D_L values were smaller than D_E values for most solutes tested in this study (Table IV). This decreased diffusivity within the gel over time could be due to the decreased concentration gradient between release media and sIPN matrix, or the increased transport pathway for solutes resided in the bulk of the sIPN disks. In the early stage of release study, most of the drug molecules will stay in the bulk of sIPN matrix and as a result,
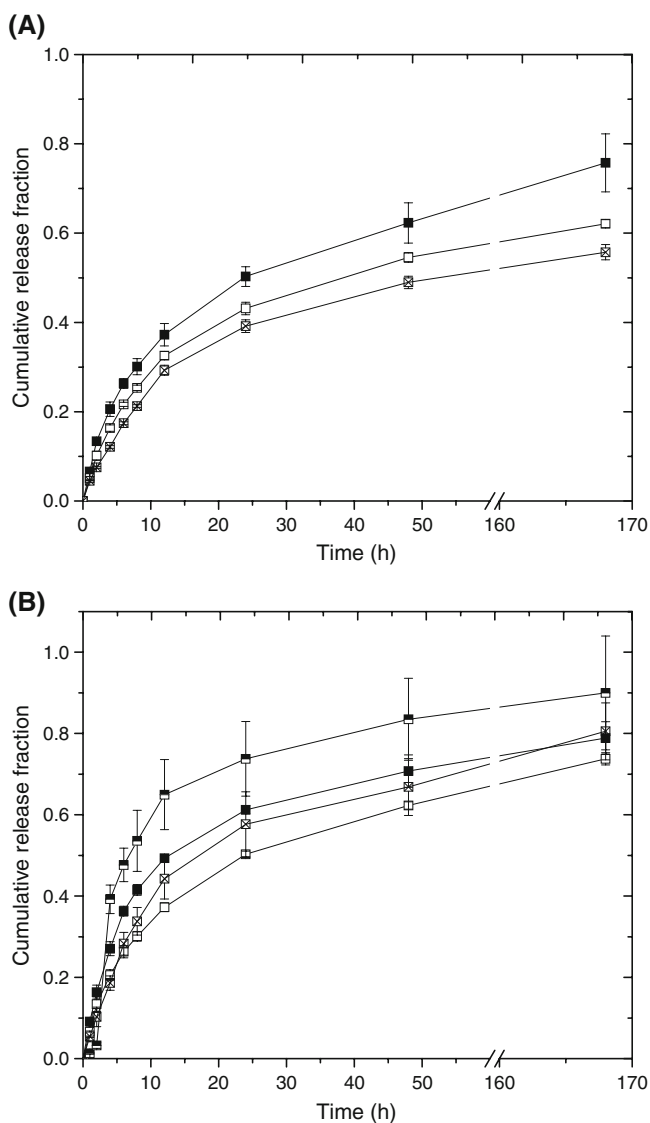
(A)

(B)

Fig. 5. (A) Effects of PEGdA content on BSA-FITC release from sIPNs, sIPN of gelatin/PEGdA w/w ratios 10:15 (——■——), 10:20 (——□——), 10:30 (——⊠——). (B) Effects of gelatin content on BSA-FITC release from sIPNs and PEG-only hydrogels, 15% w/v PEG-only hydrogel (——■——), sIPN of gelatin/PEGdA w/w ratios 10:15 (——□——), 15:15 (——⊠——), 20:15 (——■——). Data represented as average ± S.D. (n=3).

a higher concentration gradient would be expected. While in the late-time stage, the bulk concentration will decrease due to continuous release of solutes and the concentration gradient will keep decreasing until it reaches equilibrium. At the equilibrium, the concentration gradient approaches zero and there will be no driving force for solute transport. As shown in the release graph, the release curve reaches a plateau in the late-time stage. This is why smaller late-time diffusivity (D_L) values were observed using late-time release data. The sIPNs prepared with higher PEGdA content exhibited a lower diffusion coefficient derived from both early-time and late-time equations. This reduction in diffusivity might be due to the smaller mesh size as a result of increased crosslinking density. According to the Stokes-Einstein equation, decreased diffusivity can be explained by the increased viscosity inside the sIPN matrix or by the increased Stokes radius of the solute. However, sIPNs prepared with higher gelatin content showed a higher diffusion coefficient. Due to the effect of gelatin dissolution, solutes would possibly diffuse out of the matrix along with gelatin molecules. On the other hand, gelatin dissolution may generate more free volume inside the gel matrix, increasing the potential pathways for solute transport.

Release data from various sIPN formulations and PEG-only hydrogels (0–24 h) were fit to Eq. 3, and the diffusional exponents, n, are listed in Table V. SD or AgSD and BSA-FITC release from most sIPN formulations had n-values closer to 0.5, indicating Fickian diffusion. Bup, NaSD and KGF had n-values less than 0.5, which suggests anomalous release profiles. However, one important trend was the increase of the diffusional exponent with increasing PEGdA content. With the assumption that increasing PEGdA content would lead to increased degree of crosslinking, the results in this study corresponded well with others' findings (15). The power law exponent with varying gelatin content did not show any noticeable trend which made these material systems particularly interesting for further study.

The early- and late-time equations are derived from the Fickian diffusion equation for one-dimensional solute transport. However, the actual transport mechanism may not be pure Fickian diffusion driven as discussed above. Therefore, the determination of intra-gel diffusivity in this study is a rough estimation and could provide some insight into the relationship between solute diffusivity and the sIPN material system.

Table IV. Diffusion Coefficients of Model Compounds in sIPNs and PEG-only Hydrogels at 37°C

		D (×10^{-8}cm^2/s)											
		Early-time (0–6 h)						Late-time (6–24 h)					
Solute	Type of loading	1[a]	2[a]	3[a]	4[a]	5[a]	6[a]	1[a]	2[a]	3[a]	4[a]	5[a]	6[a]
AgSD	Single	1.760	1.680	1.640	1.670	2.640	0.972	1.647	0.987	0.745	1.869	3.307	1.112
	Concurrent	2.900	2.026	2.052	1.540	1.170	0.645	0.642	0.888	0.812	1.228	0.494	0.325
Bup	Single	4.250	3.829	3.649	4.180	4.620	2.75	1.480	0.787	0.895	2.480	1.534	0.096
	Concurrent	4.394	3.841	3.878	4.080	3.950	2.12	1.38	1.20	0.827	1.193	2.028	0.094
NaSD	Single	2.560	2.560	1.530	-	-	3.18	1.13	1.19	0.675	-	-	1.6
KGF	Single	0.060	0.005	0.001	0.085	0.092	0.001	7.1×10^{-3}	5.2×10^{-3}	3.9×10^{-3}	0.018	5.1×10^{-3}	1.2×10^{-3}
BSA-FITC	Single	0.333	0.234	0.155	0.412	1.310	0.63	0.155	0.131	0.110	0.225	0.331	0.23

[a], sIPN of gelatin/PEGdA w/w: 1, 10:15; 2, 10:20; 3, 10:30; 4, 15:15; 5, 20:15. 6, PEG-only hydrogel of 15% w/v PEGdA.

Table V. Diffusion Exponents, n, for Drug Release in PBS at 37°C From sIPNs and PEG-only Hydrogels

Solute	Type of loading	1[a]	2[a]	3[a]	4[a]	5[a]	6[a]
AgSD	Single	0.537	0.531	0.561	0.598	0.448	0.644
	Concurrent	0.379	0.445	0.440	0.449	0.440	0.434
Bup	Single	0.124	0.166	0.200	0.189	0.208	0.113
	Concurrent	0.118	0.150	0.160	0.162	0.191	0.125
NaSD	Single	0.139	0.165	0.178	-	-	0.081
KGF	Single	0.193	0.313	0.044	0.102	0.242	0.18
BSA-FITC	Single	0.524	0.555	0.622	0.605	0.545	0.483

[a], sIPN of gelatin/PEGdA w/w: 1, 10:15; 2, 10:20; 3, 10:30; 4, 15:15; 5, 20:15. 6, PEG-only hydrogel of 15% w/v PEGdA.

Diffusion Model Fit

There are three main theories that were successfully applied to explain experimental diffusivity data in either heterogeneous or homogeneous gel systems. Therefore, both D_E/D_0 and D_L/D_0 were fit to following hydrogel-based diffusion models to explain the solute diffusion within sIPNs.

Lustig and Peppas's Free Volume Model. Based on the free volume theory, solutes pass through the polymer chains only if their effective radius is smaller than the scaling correlation length between crosslinks (16,23). In Eq. 7, φ represents the volume fraction of polymer in the gel. D_0 is estimated by the diffusion coefficient of the solute in water. r_s denotes the hydrodynamic radius of solute. k_1 and k_2 accounts for undefined structural constants for a given polymer-solvent system.

$$\frac{D_g}{D_0} = \left(1 - k_1 r_s \varphi^{0.75}\right) \exp\left(-k_2 r_s^2 \left(\frac{\varphi}{1-\varphi}\right)\right) \quad (7)$$

Cukier's Hydrodynamic Model. Based on the Stokes-Einstein equation, hydrodynamic model describes solute transport through gels with the assumption that polymer chains enhance the frictional drag on the solute by slowing down the fluid near the polymer chain (16,24). In Eq. 8, k_c is an undefined constant for a given polymer-solvent system.

$$\frac{D_g}{D_0} = \exp\left(-k_c r_s \varphi^{0.75}\right) \quad (8)$$

Ogston's Obstruction Model. Assuming that the presence of impenetrable polymer chains causes an increase in the diffusion path length (16,25), Ogston's obstruction model takes into account the probability of the solute to find enough space between polymer fibers allowing its passage, while hydrodynamic interactions between the mobile solute and the polymer matrix are neglected (26). In Eq. 9, r_f is the radius of the polymer fiber.

$$\frac{D_g}{D_0} = \exp\left[-\frac{(r_s + r_f)}{r_f}\sqrt{\varphi}\right] \quad (9)$$

All three models achieved a relatively good fit with release data from sIPNs of varying PEGdA weight percent-

Table VI. Regression Results of Diffusion Models Applied to Solute Diffusion in sIPN

Solute	Type of loading	Early-time (0–6 h)							Late-time (6–24 h)						
		Lustig-Peppas			Cukier		Ogston		Lustig-Peppas			Cukier			
		k_1	k_2	R^2	k_c	R^2	r_f (Å)	R^2	k_1	k_2	R^2	k_c	R^2	r_f (Å)	R^2
(A) Varying PEGdA weight percentage															
AgSD	Single	0	0.28	0.8966	2.07	0.9733	1.41	0.9884	0	0.28	0.9590	2.06	0.9595	1.39	0.9701
	Concurrent	0	0.26	0.9086	1.96	0.9796	1.32	0.9923	0	0.32	0.8850	2.36	0.9663	1.63	0.9835
Bup	Single	0	0.35	0.9021	2.17	0.9762	1.46	0.9903	0	0.45	0.9097	2.79	0.9798	1.92	0.9921
	Concurrent	0	0.35	0.8997	2.16	0.9751	1.45	0.9896	0	0.45	0.9180	2.75	0.9837	1.90	0.9949
NaSD	Single	0	0.45	0.8380	2.70	0.9505	1.82	0.9806	0	0.52	0.8383	3.09	0.9512	2.11	0.9811
KGF	Single	0	0.05	0.9723	1.18	0.9965	0.84	0.9920	0	0.05	0.9098	1.19	0.9800	0.85	0.9927
BSA-FITC	Single	0	0.01	0.9298	0.37	0.9890	0.25	0.9976	0	0.01	0.9092	0.41	0.9797	0.28	0.9925
(B) Varying gelatin weight percentage															
AgSD	Single	0	0.29	0.8666	2.14	0.9557	1.47	0.9758	0	0.21	0.8254	1.57	0.9188	1.03	0.9383
	Concurrent	0	0.30	0.8503	2.22	0.9453	1.53	0.9678	0	0.34	0.8132	2.53	0.9226	1.77	0.9495
Bup	Single	0	0.36	0.8676	2.23	0.9569	1.50	0.9769	0	0.42	0.5084	2.80	0.6798	1.97	0.7326
	Concurrent	0	0.37	0.8520	2.30	0.9477	1.56	0.9699	0	0.55	0.7507	3.50	0.8776	2.48	0.9111
NaSD	Single	-	-	-	-	-	-	-	-	-	-	-	-	-	-
KGF	Single	0	0.05	0.6729	1.07	0.7969	0.74	0.8518	0	0.06	0.8018	1.33	0.9005	0.94	0.9390
BSA-FITC	Single	0	0.01	0.8042	0.34	0.9086	0.22	0.9443	0	0.01	0.8380	0.41	0.9318	0.27	0.9059

Data represented as the average of three replicate studies.

age, with R^2 values near or above 0.9 (Table VIA, B). Assuming no degradation of the network D_E/D_0 or D_L/D_0 *vs.* the polymer volume fraction (φ) could be well modulated by these models. Ogston's obstruction model showed relatively better fit with all model solutes. Though based on different theories, the three equations above were all in the exponential decay form. Compared to others' findings, the polymer volume fractions tested in this study were relatively big, and the data points were all at the tail end of the exponential decay curve (16). Changes in φ did not lead to significant changes in D_E/D_0 or D_L/D_0, and the curve fit results for sIPNs with varying gelatin weight percentages did not fail completely (Table VIB), even though the trend with sIPNs of varying gelatin weight percentages contradicted with what the theoretical model predicted. The theoretical models predict increasing the polymer volume fraction will decrease free volume within the gel matrix and thus lead to decreased diffusivity. However, the *in vitro* release results of sIPNs showed initial release rate and intra-gel diffusivity increased with increasing gelatin content.

DISCUSSIONS

Single-loaded AgSD and Bup retained their unique shape of release curves in all sIPN formulations. For AgSD, near zero-order release kinetics was observed in the first 8 or 12 h. For Bup, the release curves obtained from sIPNs, PEG-only hydrogels and gelatin-only hydrogels all displayed first-order kinetics. These results suggest that the release patterns of AgSD and Bup (*i.e.* release order) were less influenced by the formulations than by solute physicochemical properties. AgSD had very low water solubility ($K_{sp}=8\times10^{-12}$ at pH 7 and 25°C) (27) and as a result, the ionization of SD group appeared to be the release rate controlling step. On the contrary, Bup had good water solubility and displayed a significant 'burst effect'. This burst release could be either due to the specific drug property or the heterogeneity of the polymer matrices (28). Serra and Peppas revealed that the incorporated solvent during polymerization greatly affected the release kinetics, which decreased the formation of crosslinks and led to heterogeneous networks (29). As the solvent for gelatin, water was incorporated during sIPN polymerization, and as a result, it might lead to a non-homogeneous structure and burst release. mPEG-modified sIPN showed more significant burst release than unmodified sIPN. As the gelatin backbone was modified with PEG linkers, the sIPN matrix had more PEG chain entanglements. These hydrophilic PEG linkers may be on the surface of the matrix forming a brush-like structure, creating more free space for solute transport, and the overall hydrophilicity of the system is increased. For most of the sIPN formulations, the concurrent loading of AgSD and Bup into various sIPN matrices did not change their overall release behaviors, indicating no strong interaction between SD and Bup exists within the sIPN matrices of varying formulations. The similarity between NaSD and Bup release profile might be explained by the water solubility and comparable molecular size. Water solubility renders the molecule more likely to be associated with the PEG-brushes on the sIPN surface, leading to the 'burst effect'. Small molecular size suggests they are not likely to be trapped in microregions of the interpenetrating matrices. The release of NaSD depended on PEGdA content in PBS, while this trend was less observed in RPMI 1640.

In contrast to the low cumulative release of KGF, the maximum cumulative release percentage of BSA-FITC reached above 50% for all formulation groups. One of the major reasons behind this difference might be the differences in loading amount. The loading amount of BSA-FITC per disk was 10^5-fold higher than that of KGF. One hypothesis is the free thiol groups in cysteine residues may react with acrylate groups via Michael-type addition (30). Due to the small loading amount of KGF (10 ng per disk), most of the KGF might react with the acrylate groups, resulting in the formation of covalent bond with PEG matrices or conformational changes and the extremely low cumulative release percentage. The greater amount of BSA-FITC loaded most likely saturated free acrylate groups inside the PEG matrices with most of the BSA-FITC free to diffuse out of the sIPN matrices in a controlled manner. In addition, the interaction between proteins and free radicals generated during photopolymerization may lead to irreversible immobilization of the protein during network formation. A study revealed that when increasing the loading amount of albumin, the maximum cumulative release has been greatly increased but the amount of unreleased protein within each of these photopolymerized hydrogel networks remains relatively constant (31).

In short, various contributing factors impacted the release kinetics of model solutes from sIPN matrices, such as gelatin and PEGdA content, molecular size, solute water solubility. Any factor that reduces the size of water-filled spaces inside the gel matrix should have an effect on the solute transport. Such factors include the solute size in relation to the opening size between polymer chains and polymer chain mobility (26). Thus, the polymer weight percentage was varied in the sIPN to yield different formulations, and the release profiles of solutes of different sizes were also investigated. A relationship between the decreased solute diffusivity and the increased PEGdA weight percentage was observed due to the increased crosslinking density. In addition, the gelatin weight percentage was varied while keeping the PEGdA weight percentage constant. Increasing the gelatin weight percentage led to an increased cumulative fractional release, which contradicted with the polymer volume theory. According to the polymer volume theory, the polymer volume of sIPN formulation is greater than that of PEG-only hydrogel, and as a result, the sIPN should have smaller free volume and slower release rate. Pokhade *et al* studied the release kinetics of chlorothiazide from a semi-interpenetrating network composed of crosslinked chitosan and hydroxypropyl cellulose, which also revealed that diffusion coefficients decreased with increasing crosslinking density, but increased with increasing the content of non-crosslinked hydroxypropyl cellulose (32). Therefore, the polymer volume theory-based solute transport mechanism does not apply to the non-crosslinked polymer system. A degradation- or dissolution-controlled mechanism needs to be taken into account. In polymeric delivery systems displaying biphasic release kinetics, the first phase is generally considered as diffusion driven and the second phase to be controlled by degradation (33). Thus, the diffusion model alone was unable to explain the release kinetics of solutes from the sIPNs with varying gelatin weight percentage due to gelatin

dissolution effect. Furthermore, previous studies on the swelling effect of sIPNs demonstrated increased swelling ability with increased gelatin weight percentage (1). As a result, solute release kinetics from sIPNs with higher gelatin content showed anomalous release kinetics influenced by both swelling and diffusion.

CONCLUSION

Gelatin- and PEGdA-based sIPNs were synthesized for the delivery of model drugs and proteins. The study showed that both the polymer weight/volume fraction and the physicochemical properties of model compounds affected the solute release behavior. The release rate is inversely proportional to PEG content while proportional to gelatin content. However, the release order of model compounds from sIPNs seemed to depend more on the drug properties, such as water solubility and size, than on polymer composition. Mathematical analysis showed that diffusion coefficients of model solutes within the sIPNs decreased with increasing PEGdA fraction but increased slightly with increasing gelatin weight percentage. Power fit analysis revealed that AgSD and BSA-FITC transport from sIPNs was mainly Fickian diffusion-driven, while for the other model solutes, the mechanism of solute transport was anomalous, which could be due to various factors, including swelling, polymer chain relaxation, and material degradation.

ACKNOWLEDGMENTS

REFERENCES

1. Burmania JA, Kao WJ. Cell interaction with protein-loaded interpenetrating networks containing modified gelatin and poly (ethylene glycol) diacrylate. Biomaterials. 2003;24:3921–30.
2. Witte RP, Kao WJ. Keratinocyte-fibroblast paracrine interaction: the effects of substrate and culture condition. Biomaterials. 2005;26:3673–82.
3. Sperling LH. Interpenetrating polymer networks and related materials. New York: Plenum; 1981. p. 265.
4. Burmania JA, Martinez-Diaz GJ, Kao WJ. Synthesis and physicochemical analysis of interpenetrating networks containing modified gelatin and poly(ethylene glycol) diacrylate. J Biomed Mater Res A. 2003;67:224–34.
5. Zilinski J, Kao WJ. Tissue adhesiveness and host response of *in situ* photopolymerizable interpenetrating networks containing methylprednisolone acetate. J Biomed Mater Res A. 2004;68: 392–400.
6. Chung AS, Gao Q, Kao WJ. Macrophage matrix metalloproteinase-2/-9 gene and protein expression following adhesion to ECM-derived multifunctional matrices via integrin complexation. Biomaterials. 2007;28:285–98.
7. Einerson NJ, Stevens KR, Kao WJ. Synthesis and physicochemical analysis of gelatin-based hydrogels for drug carrier matrices. Biomaterials. 2003;24:509–23.
8. Witte RP, Blake AJ, Palmer C, Kao WJ. Analysis of poly (ethylene glycol)-diacrylate macromer polymerization within a multicomponent semi-interpenetrating polymer network system. J Biomed Mater Res A. 2004;71:508–18.
9. Waldeck H, Chung AS, Kao WJ. Interpenetrating polymer networks containing gelatin modified with PEGylated RGD and soluble KGF: synthesis, characterization, and application in *in vivo* critical dermal wound. J Biomed Mater Res A. 2007;82:861–71.
10. Kleinbeck KR, Faucher L, Kao WJ. Multifunctional *in situ* photopolymerized semi-interpenetrating network system is an effective donor site dressing: a cross comparison study in a swine model. J Burn Care Res. 2008;30:37–45.
11. Serra L, Domenech J, Peppas NA. Drug transport mechanisms and release kinetics from molecularly designed poly(acrylic acid-g-ethylene glycol) hydrogels. Biomaterials. 2006;27:5440–51.
12. United States Pharmacopeia and National Formulary USP 26 - NF 21. The United States Pharmacopeial Convention, Inc., Rockville, MD; 2003. pp. 1728.
13. United States Pharmacopeia and National Formulary USP 26 - NF 21. The United States Pharmacopeial Convention, Inc., Rockville, MD; 2003. pp. 276.
14. United States Pharmacopeia and National Formulary USP 26 - NF 21. The United States Pharmacopeial Convention, Inc., Rockville, MD; 2003. pp. 1731.
15. Gilchrest BA, Marshall WL, Karassik RL, Weinstein R, Maciag T. Characterization and partial purification of keratinocyte growth factor from the hypothalamus. J Cell Physiol. 1984;120:377–83.
16. Amsden B. Solute diffusion within hydrogel: mechanisms and models. Macromolecules. 1998;31:8382–95.
17. Bult A, Plug CM. Silver sulfadiazine, In: Analytical Profiles of Drug Substances. *American Pharmaceutical Association.* 1984;13:553–71.
18. Brazel CS, Peppas NA. Mechanisms of solute ad drug transport in relaxing, swellable, hydrophilic glassy polymers. Polymers. 1999;40:3383–98.
19. Ritger PL, Peppas NA. A simple equation for description of solute release I. Fickian and non-Fickian release from non-swellable devices in form of slabs, sphere, cylinders or discs. J Control Release. 1987;5:23–36.
20. Amsden B. Diffusion in polyelectrolyte hydrogels: application of an obstruction-scaling model to solute diffusion in calcium alginate. Macromolecule. 2001;34:1430–5.
21. Bader RA, Herzog KT, Kao WJ. Mass transport properties of gelatin-based semiinterpenetrating networks for use in wound healing. Polym Bull. 2009;62:367–80.
22. Amsden B. An obstruction scaling model for diffusion in homogeneous hydrogels. Macromolecules. 1999;32:874–9.
23. Lustig SR, Peppas NA. Solute diffusion in swollen membranes. J Appl Polym Sci. 1988;36:735–47.
24. Cukier RI. Diffusion of brownian spheres in semidilute polymer solutions. Macromolecules. 1984;17:252–5.
25. Ogston AG. The spaces in a uniform random suspension of fibres. Trans Faraday Soc. 1958;54:1754–7.
26. Amsden B. Solute diffusion in hydrogels. An examination of retardation effect. Polymer Gels and Networks. 1998;6:13–43.
27. Nesamony J, Kolling WM. IPM/DOSS/Water microemulsions as reactors for silver sulfadiazine nanocrystal synthesis. J Pharm Sci. 2005;94:1310–20.
28. Huang X, Brazel CS. On the importance and mechanisms of burst release in controlled drug delivery — a review. J Control Release. 2001;73:121–36.
29. Serra L, Domenech J, Peppas NA. Drug transport mechanisms and release kinetics from molecularly designed poly(acrylic acid-g-ethylene glycol) hydrogels. Biomaterials. 2006;27:5440–51.
30. Lutolf MP, Tirelli N, Cerritelli S, Cavalli L, Hubbell JA. Systematic modulation of Michael-type reactivity of thiols through the use of charged amino acids. Bioconjug Chem. 2001;12:1051–6.
31. Lin CC, Metters AT. Enhanced protein delivery from photopolymerized hydrogels using a pseudospecific metal chelating ligand. Pharm Res. 2006;23:614–22.
32. Rokhade AP, Kulkarni PV, Mallikarjuna NN, Aminabhavi TM. Preparation and characterization of novel semi-interpenetrating polymer network hydrogel microspheres of chitosan and hydroxypropyl cellulose for controlled release of chlorothiazide. J Microencapsul. 2009;26:27–36.
33. Lin CC, Metters AT. Hydrogels in controlled release formulations: network design and mathematical modeling. Adv Drug Deliv Rev. 2006;58:1379–408.